Supplementary Information: Optimizing $CuFeS_2$ Chalcopyrite Thin Film Synthesis: A Comprehensive Three-Step Approach Using Ball-Milling, Thermal Evaporation, and Sulfurization Applied for Thermoelectric Generation

Marcelo Augusto Malagutti[a], Ketan Lohani[a], Mirco D'Incau[a], Himanshu Nautiyal[a], Narges Ataollahi[a], and Paolo Scardi[a*]

[a] *Department of Civil, Environmental and Mechanical Engineering, University of Trento, via Mesiano 77,38123 Trento, Italy.*

*Corresponding author

E-mail address: paolo.scardi@unitn.it

Supplementary Note S1: Parameters of Synthesis of CFS

Table S 1. FeCu milling parameters.

Sample Identifier	Atomic Proportion (Cu:Fe)	Milling Time (h)	Lubricant
FeCu-01	1:1	2	None
$Fe_{1.76}$Cu-02	1:1.76	2	None
FeCu-03	1:1	3	6% weight ethanol

Table S2. Thermal evaporation of FeCu powders.

Sample Identifier	Milled Powder	Powder Mass (g)	Target Distance (cm)	Current Ramp	Pressure (mBar)	Surface
1	Not Milled	0.215 (Fe)	27	140 A for 1h	~10^{-5}	Non-Polished
2	Not Milled	0.215 (Cu)	27	105 A for 1 h	~10^{-5}	Non-polished
3	Not milled	0.215	27	105 A for 1 h	~10^{-5}	Non-polished
4	Not milled	0.215	27	140 A for 1 h	~10^{-5}	Non-polished
5	Not milled	0.6	27	105 A to 140 steps of 5 A for 3 min each	~10^{-5}	Non-Polished
6	Not milled	0.2	9.5	105 A for 10 min +135 A for 20 s +140 for 1 min	~10^{-5}	Non-polished
7	Not milled	0.15	7.5	105 A for 3 min	~10^{-5}	Non-polished
8	Not milled	0.15	7.5	105 A for 10 min + 125 A for 20 s + 140 A for 4 min	~10^{-5}	Non-polished
9	FeCu-01	0.215	27	110 A for 5 min + 120 A for 1min15s	~10^{-5}	Non-polished

10	FeCu-01	0.06	7.5	105 A for 3 min + 130 A for 1 min	~10^{-5}	Non-polished
11	FeCu-01	0.06	7.5	105 A for 10 min + 140 A for 1 min	7×10^{-6}	Non-polished
12	FeCu-01	0.06	7.5	105 A for 10 min + 140 A for 1 min	7×10^{-6}	Non-polished
13	FeCu-01	0.06	7.5	105 A for 10 min + 140 A for 1 min	7×10^{-6}	Polished
14	$Fe_{1.76}Cu$-02	0.06	7.5	105 A for 10 min + 140 A for 1 min	7×10^{-6}	Non-Polished
15	$Fe_{1.76}Cu$-02	0.06	7.5	105 A for 10 min + 140 A for 1 min	7×10^{-6}	Polished
16	FeCu-03	0.06	7.5	105 A for 10 min + 140 A for 1 min	7×10^{-6}	Non-Polished
17	FeCu-03	0.06	7.5	105 A for 10 min + 140 A for 1 min	7×10^{-6}	Polished
18	FeCu-03	0.06	7.5	105 A for 10 min + 140 A for 1 min	7×10^{-6}	Non-Polished

Supplementary Note S2: Non-milled Cu-Fe powders optimization

Thermal evaporation of Fe and Cu elemental powders, respectively – corresponding to samples 1 and 2, formed a face-centred cubic (*fcc*) structure with the space group *Fm-3m* (Cu: ICSD # 627117; Fe: ICSD # 53803). This means that the high-temperature phase of Fe was stabilized at room temperature and with overall good crystallinity. The Rietveld refinement of the XRD patterns revealed that the as-deposited Fe thin film sample's average crystallite size (volumetric average) is about ~8 nm, half that of the Cu sample (~17 nm). Also, the Cu as-deposited film shows a preferred orientation along the [111] direction. Figures S1 and S2 of the Supplementary Note 4 show the Rietveld refinement for Cu and Fe, respectively.

For samples 3 and 4, a mixture of Fe and Cu was evaporated using a current of 105 A and 140 A, respectively. For the former, evaporation was expected to be of Cu only, although Fe was also present (see Figures S3 and S4 of Supplementary Note 4). These samples showed Fe as a major phase. As discussed in the main text, evaporation of Cu occurs

at a lower current than Fe, so it is expected that the major phase on the sample's surface is Fe. However, the possibility of Cu-Fe alloy formation is not ruled out in the refinement, although it should probably happen between the interface of Cu and Fe in the middle of the film.

To achieve better homogeneity and formation of Cu-Fe alloy, a gradual increase in current was set to start at 105 A and slowly ramp up to 140 A during the evaporation for sample 5. However, this didn't contribute to a better homogenization of the film, meaning that the Fe and Cu form separated layers, which is detrimental to the formation of a pure CFS alloy.

As a last attempt to improve the diffusion of Fe and Cu with the non-milled powders, the substrate for samples 6, 7, and 8 was positioned closer to the W boat. Sample 6 underwent a gradual current increase from 105 A to 140 A; while for sample 7, the distance to the target was further reduced, maintaining a current of 105 A (that of the Cu). In the case of sample 8, the gradual current increase was done with the same distance as sample 7. Sample 6 showed Cu (*fcc*) and Fe (*bcc*) layers and increased crystallinity compared to the previously discussed samples (observed by the sharper Bragg peaks in Figure 2(a) of the main text). Sample 7 showed only Fe. However, in sample 8, better mixing of Cu and Fe on the film was observed, where the distance between source and target was minimal (7.5 cm). For this case, a current of 105 A was applied for 10 minutes, followed by an increase to 140 A lasting 1 minute. The Rietveld refinement for all the samples is displayed in Figures S6, S7, and S8.

Supplementary Note S3: Optimization of the Ball-Milling Procedure

3.1. Effect of target distance

Here, the first comparison between milled and non-milled FeCu powders in the evaporation process is presented. The FeCu-01 sample was evaporated having the target positioned far away from the boat (27 cm) as in the first cases of the non-milled powders, using the parameters of sample 9 (*vide* Table S2 for specifics). The thermal evaporation of this sample and its sulfurization in a static Ar atmosphere are displayed in Figure 4(a) of the main text. Sample 9 showed the formation of *bcc* Fe, together with a small proportion of CuFe alloy. The introduction of sulphur via sulfurization lead to the formation of two phases,

i.e., bornite $Cu_{4.98}Fe_{1.02}S_4$ (*Pbca*, PDF # 01-071-368) and CFS chalcopyrite (PDF # 00-037-0471), the latter with preferred orientation in the [112] direction (*vide* Figure S9-bottom for the refined lattice parameters). The quantitative phase analysis (QPA) reveals that bornite and chalcopyrite are in half proportion in the sample. This can also be confirmed by the dark color aspect of the film shown in Figure S24, as chalcopyrite is known to have a golden yellow color (vide Figure 1(b) of the main text).

In the same fashion as the non-milled powders, the results proved to be better when the target was brought closer to the source. The crystallinity of sample 10 is significantly improved as evidenced by the sharpness of the Bragg peaks in Figure 4(a) when the target is positioned 7.5 cm from the source (see also Figure S10 for profile fitting). Unfortunately, this film presented poor adhesion to the substrate. To solve this problem, for sample 11, the vacuum was improved by one order of magnitude (~10^{-6} mbar) during the evaporation of the FeCu-01 powder. Another key point of this test was the lower quantity of powder employed, 0.06 g, 3 times lower than the previous sample. This increased the heating energy per gram of material.

3.2. Changing the milling parameters

Using the FeCu-01, milled for 2 h, the sulfurization of Sample 12 without polishing still presented the Bornite phase and preferred orientation for the Chalcopyrite phase along the [111] and [044] directions (see Figure 5(a) of the main text and Rietveld analysis in Figure S12). Polishing the SLG substrate for sample 13 resulted in better adhesion along with the reduction of the Bornite phase quantity in the diffractograms. However, the improvement was not adequate, and the physical aspect of the film was not satisfactory, as shown in the inset of Figure 5(a) (details in Figure S26). During the evaporation of $Fe_{1.76}$Cu-02 powders, pure chalcopyrite is formed presenting also the characteristic golden-yellow colour (see Figure S27 and inset of Figure 5(a)). In the Rietveld analysis (vide Figure S14 and S15), preferred orientation is present along [112] and [220] for sample 14, and [112] for sample 15 on the polished and non-polished substrates, respectively. The adhesion is only improved for samples 16 and 17 where the CuFe-03 powders were employed. Even with the polishing of sample 17, a better adhesion was found for sample 16 (vide Figure 5(a)), which was selected as the optimized film product.

Supplementary Note S4: Rietveld Refinement

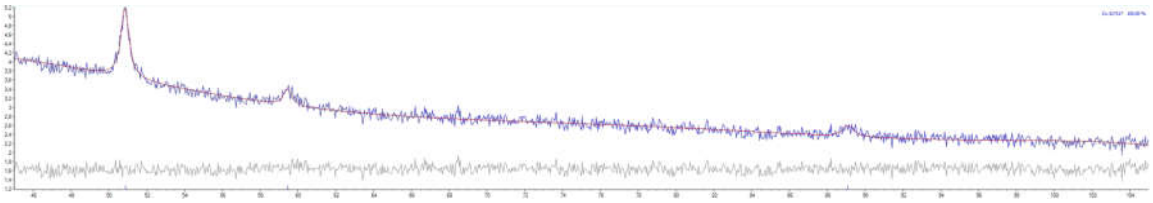

Figure S1. Sample 1.

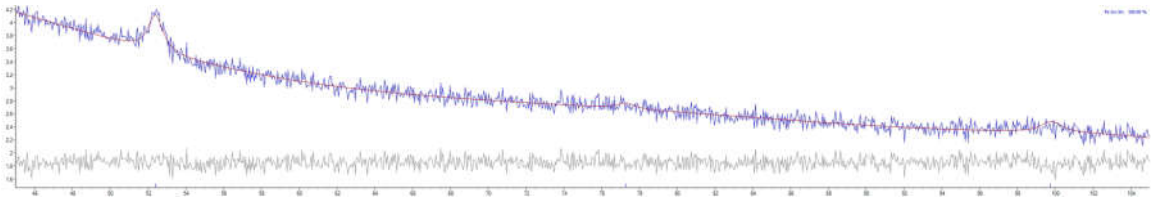

Figure S2. Sample 2.

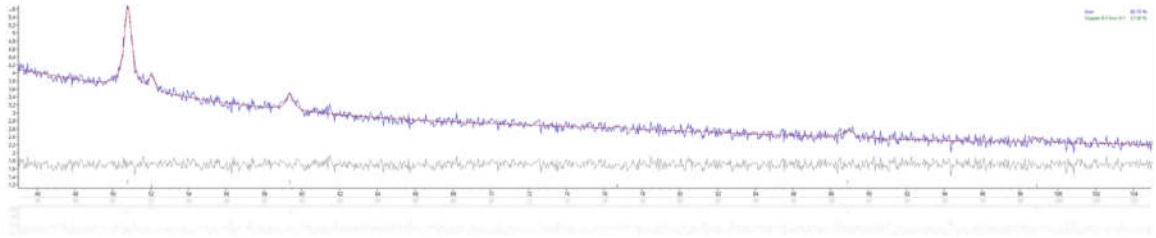

Figure S3.Sample 3

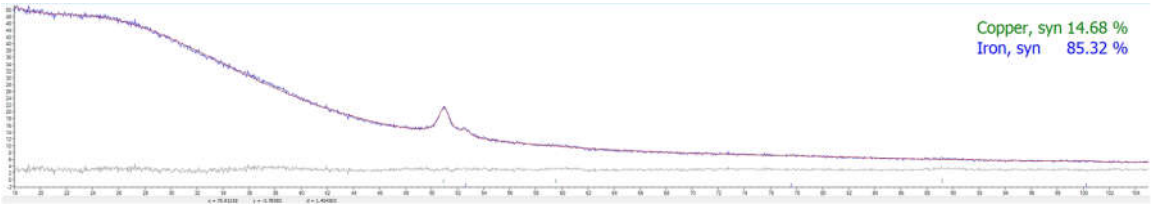

Figure S4. Sample 4.

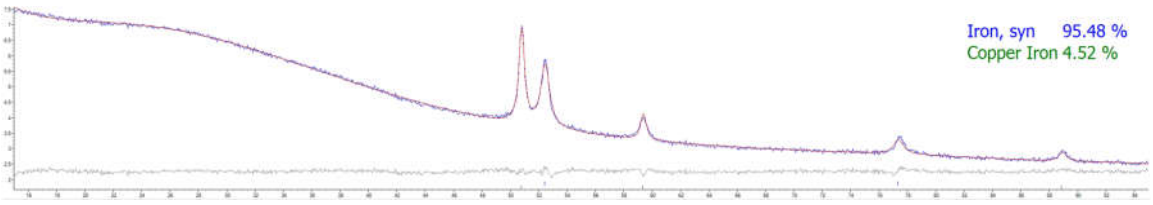

Figure S5. Sample 5.

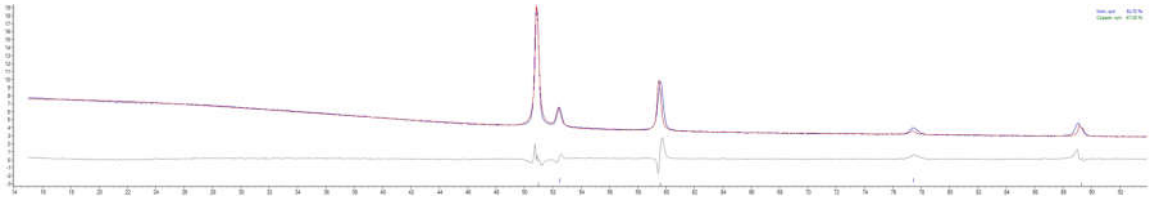

Figure S6. Sample 6. The peak shift is associated with the stress in the material.

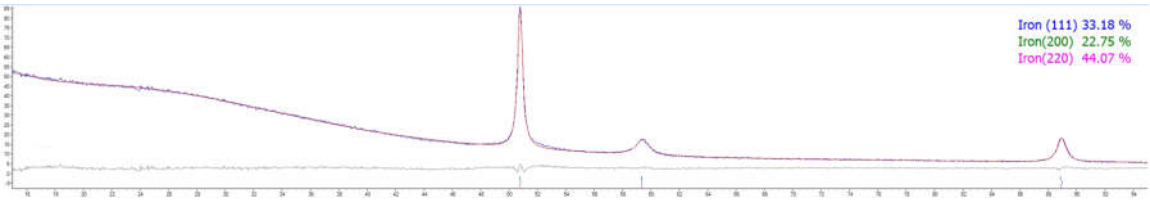

Figure S7. Sample 7.

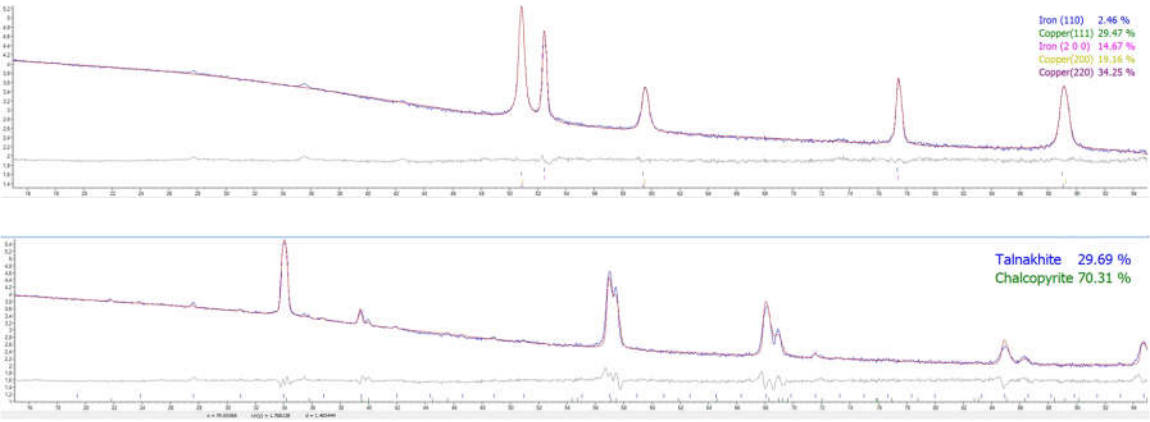

Figure S8. Sample 8 evaporated (top) and its sulfurization using the configuration 2 (bottom).

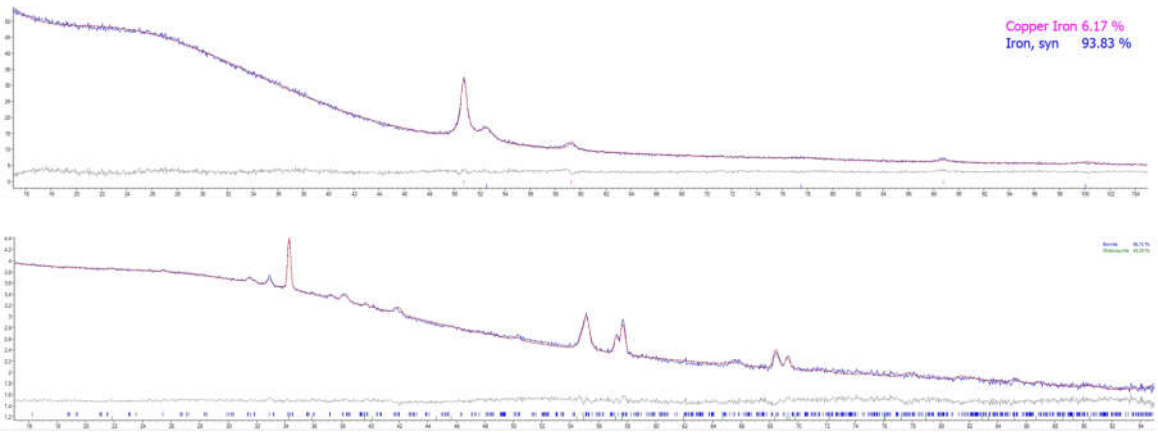

Figure S9. Sample 9 (top) and its sulfurization employing configuration 1. The lattice parameters for the Bornite phase are $a = 10.98(1)$ *Å,* $b = 21.80(9)$ *Å,* $c = 10.97(1)$ *Å, retrieved by Rietveld refinement.*

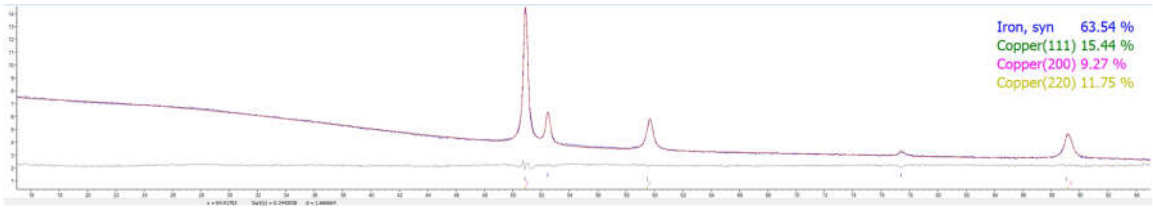

Figure S10. Sample 10

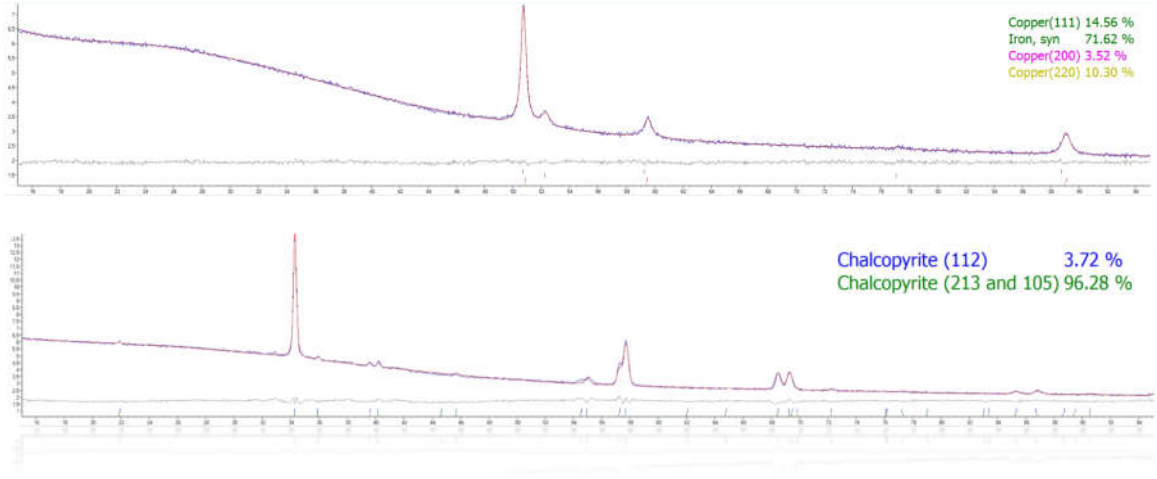

Figure S11. Sample 11 (top) and its sulfurization using setup 1.

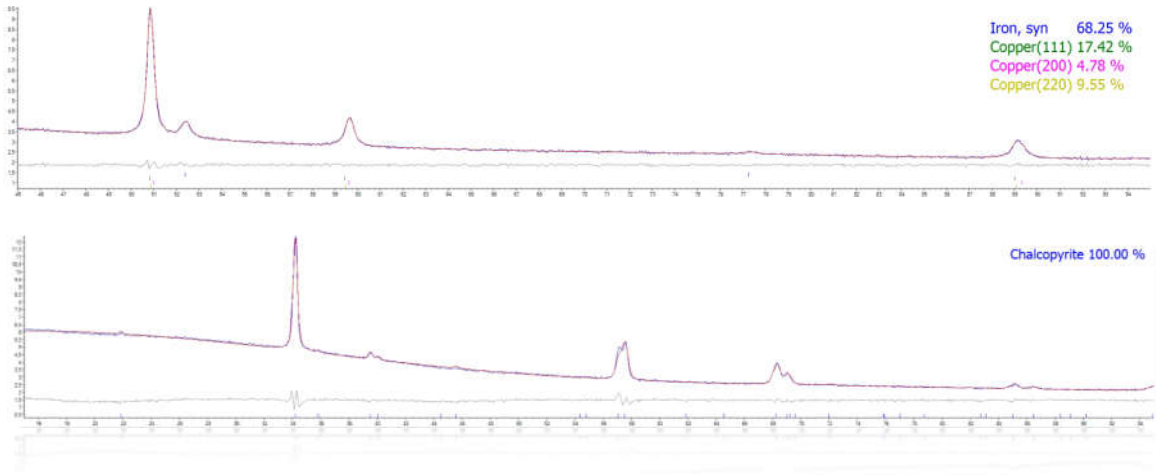

Figure S12. Sample 12 (top) and its sulfurization employing configuration 1 (bottom).

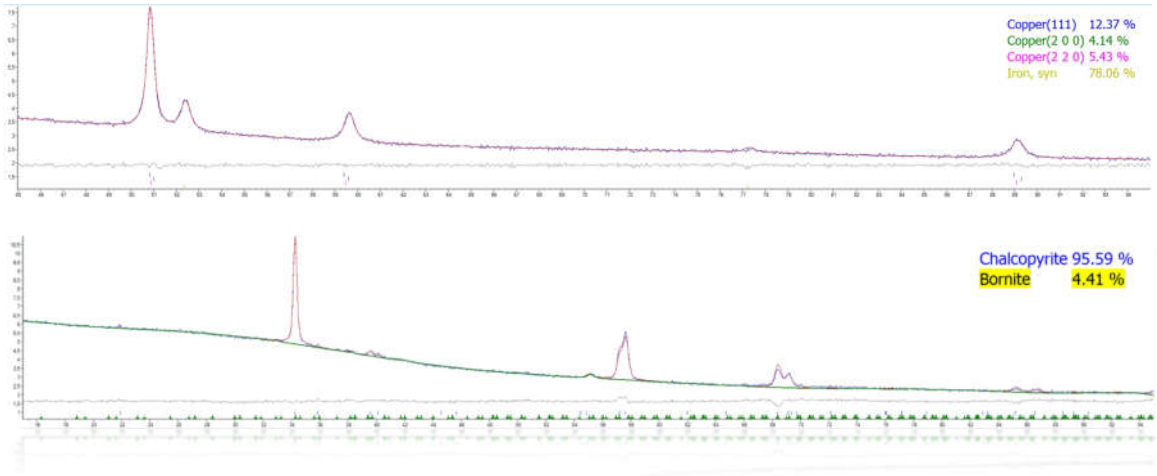

Figure S13. Sample 13 (top) and its sulfurization using configuration 2.

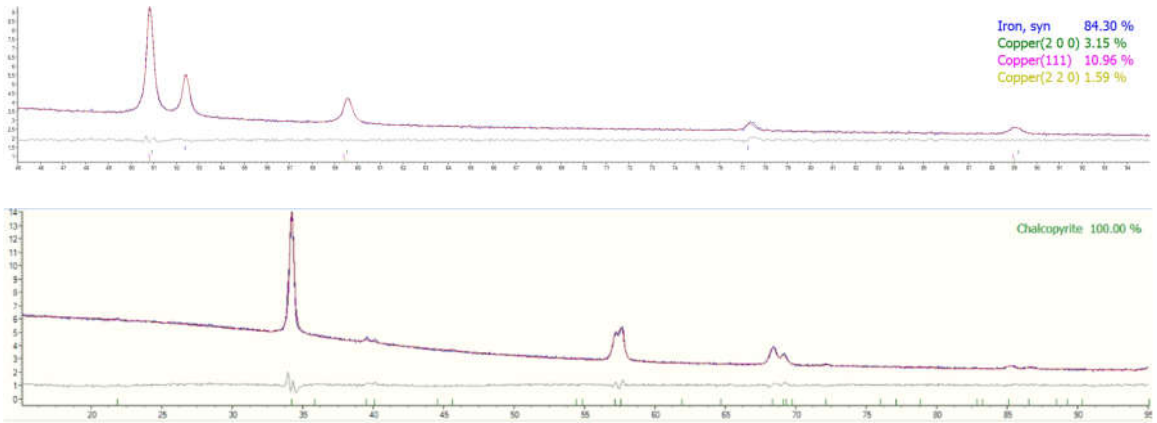

Figure S14. Sample 14 (top) and its sulfurization using configuration 2 (bottom).

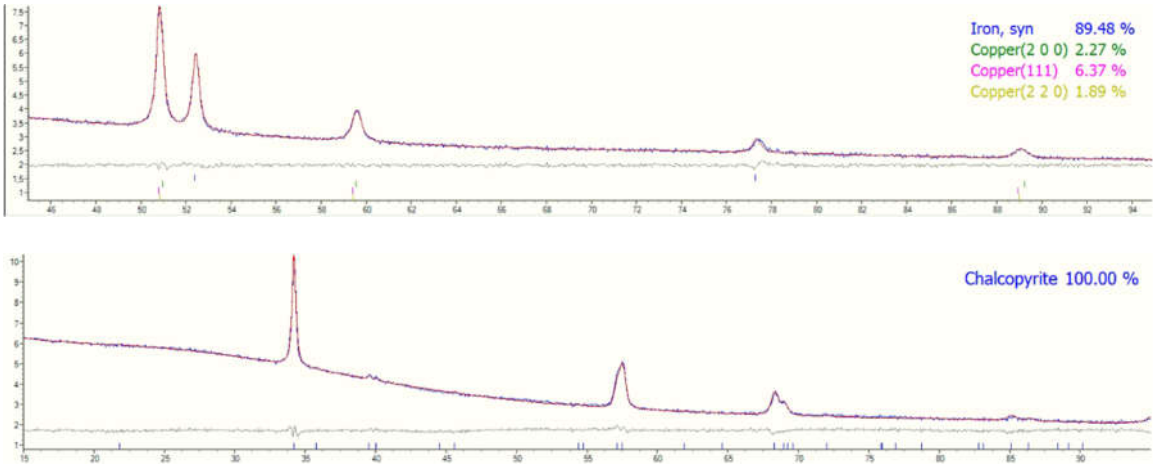

Figure S15. Sample 15 (top) and its sulfurization using configuration 2 (bottom).

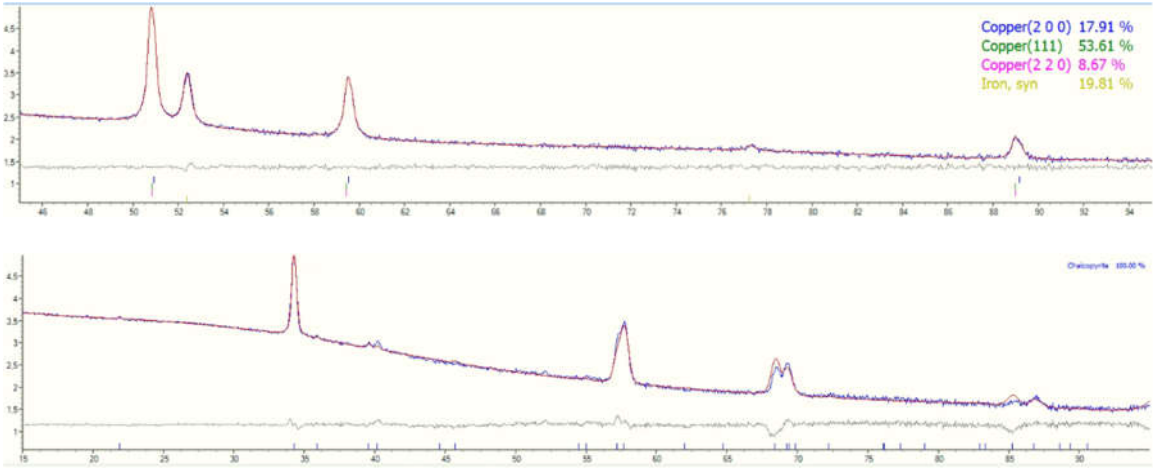

Figure S16. Sample 16 (top) and its sulfurization using configuration 2.

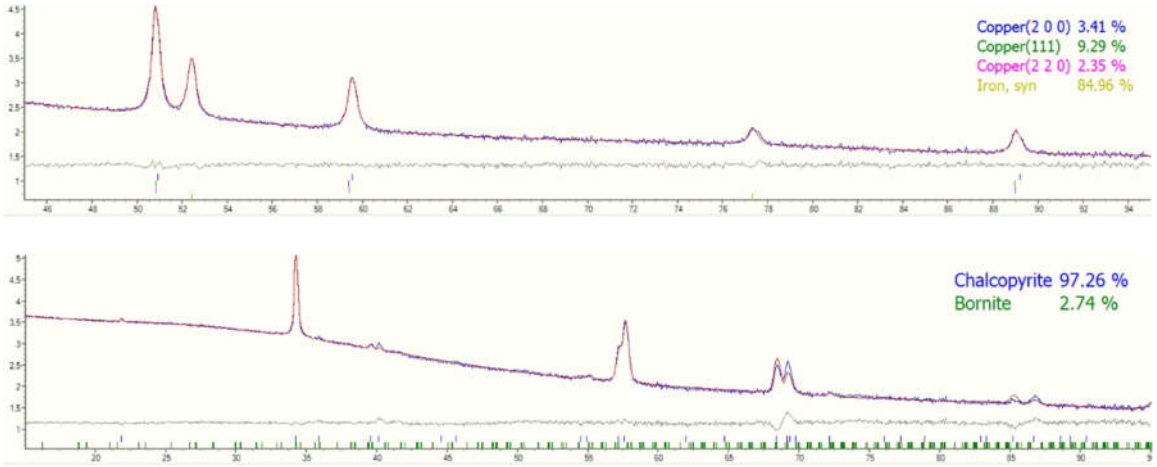

Figure S17. Sample 17 (top) and its sulfurization (bottom).

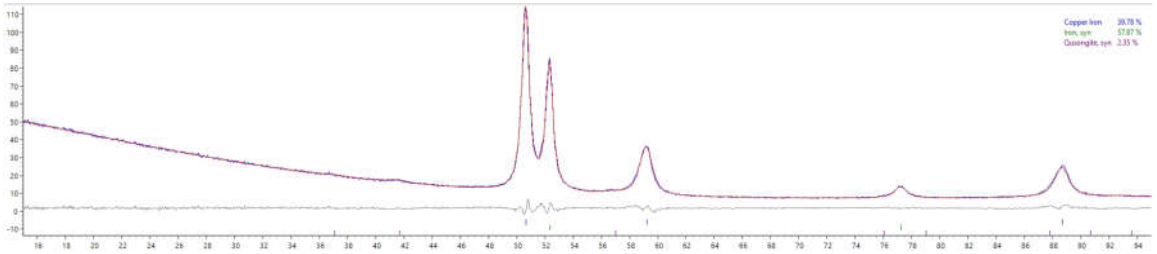

Figure S18. FeCu-01.

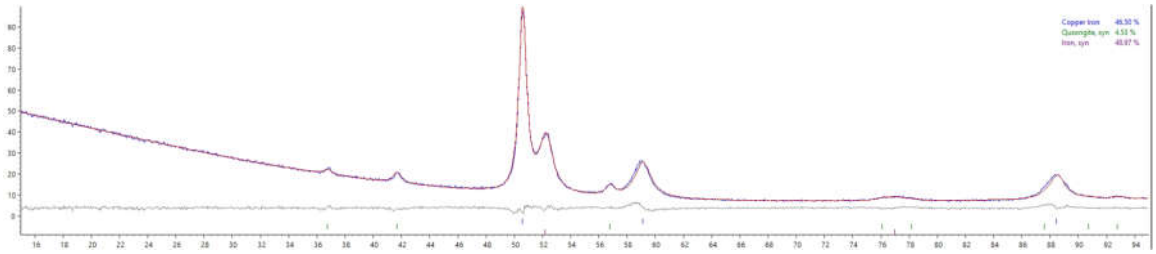

Figure S19. Fe1.76Cu-02.

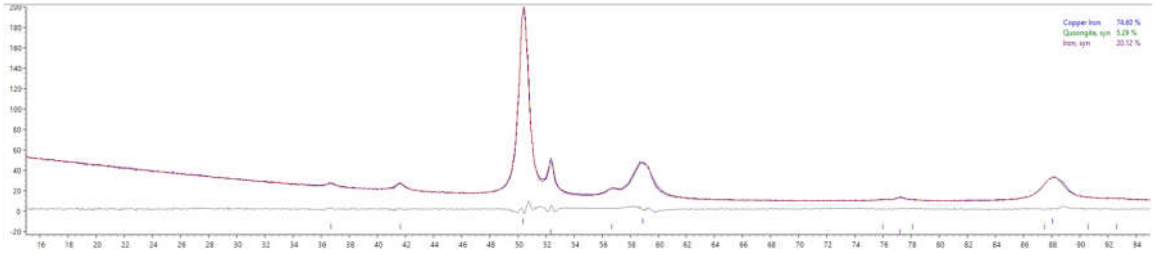

Figure S20. FeCu-03.

Supplementary Note S5: Visual inspection

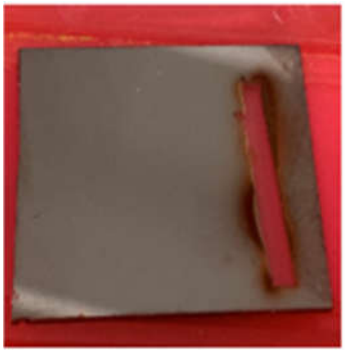

Figure S21. Samples 3.

Figure S22. Sample 4.

Figure S23. Sample 5.

Figure S24. Sample 6 after sulfurization.

Figure S25.Sample 8 sulfurized.

Figure S26. Sample 8.

Figure S27. sample 9 sulfurized

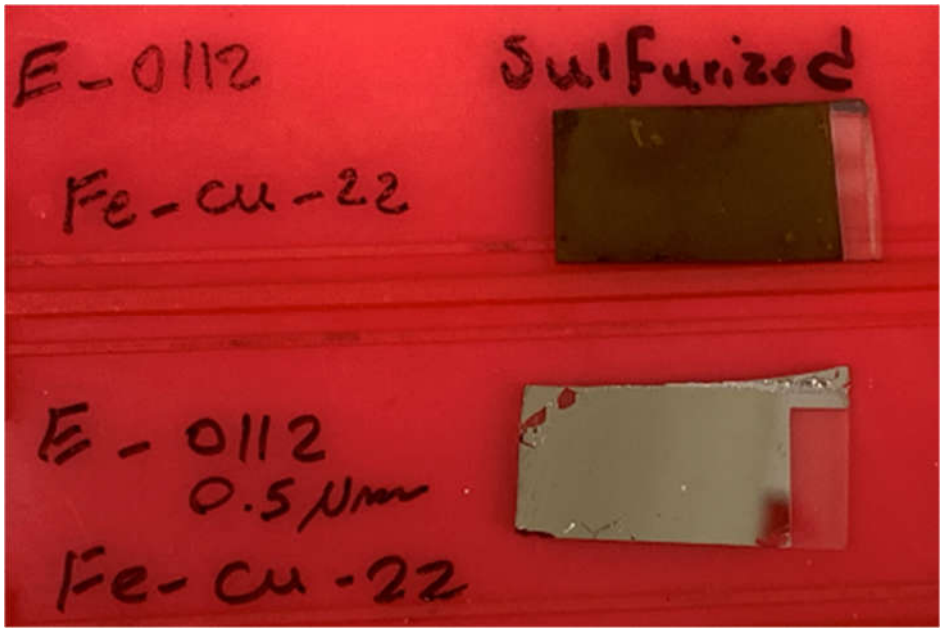

Figure S28. Sample 11.

Figure S29. Sample 12 (left-top) and 13 (right-top). Sulfurization of sample 12 (bottom).

Figure S30. Sample 14 (left-top) and 15 (right-top) and the sulfurization of sample 15 (bottom).

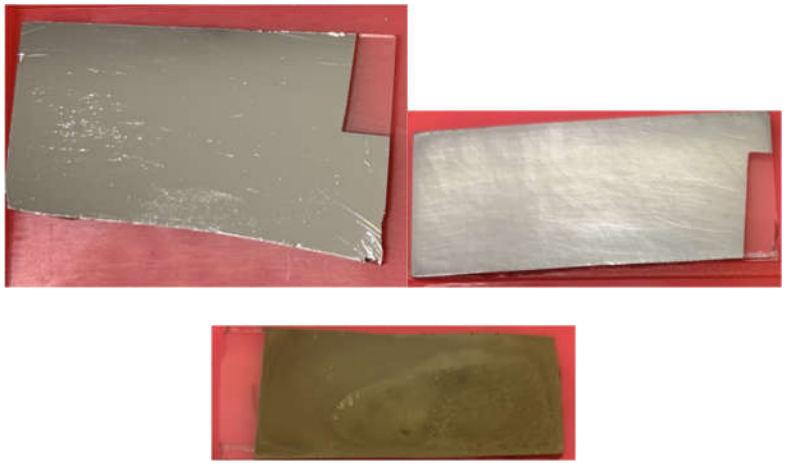

Figure S31. Sample 16 (left-top) and 17 (right-top) and the sample 16 sulfurized (bottom).

Supplementary Note S6: Comparison of different ball-milled powders

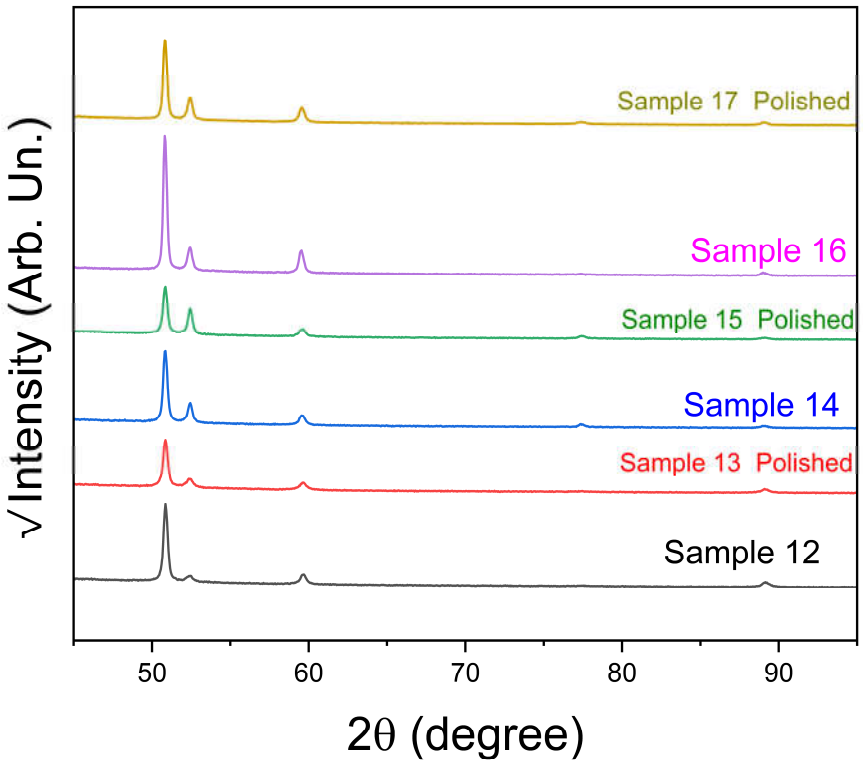

Figure S32. Diffractograms of the samples 12 to 17.

Supplemetary Note S7: Pristine film

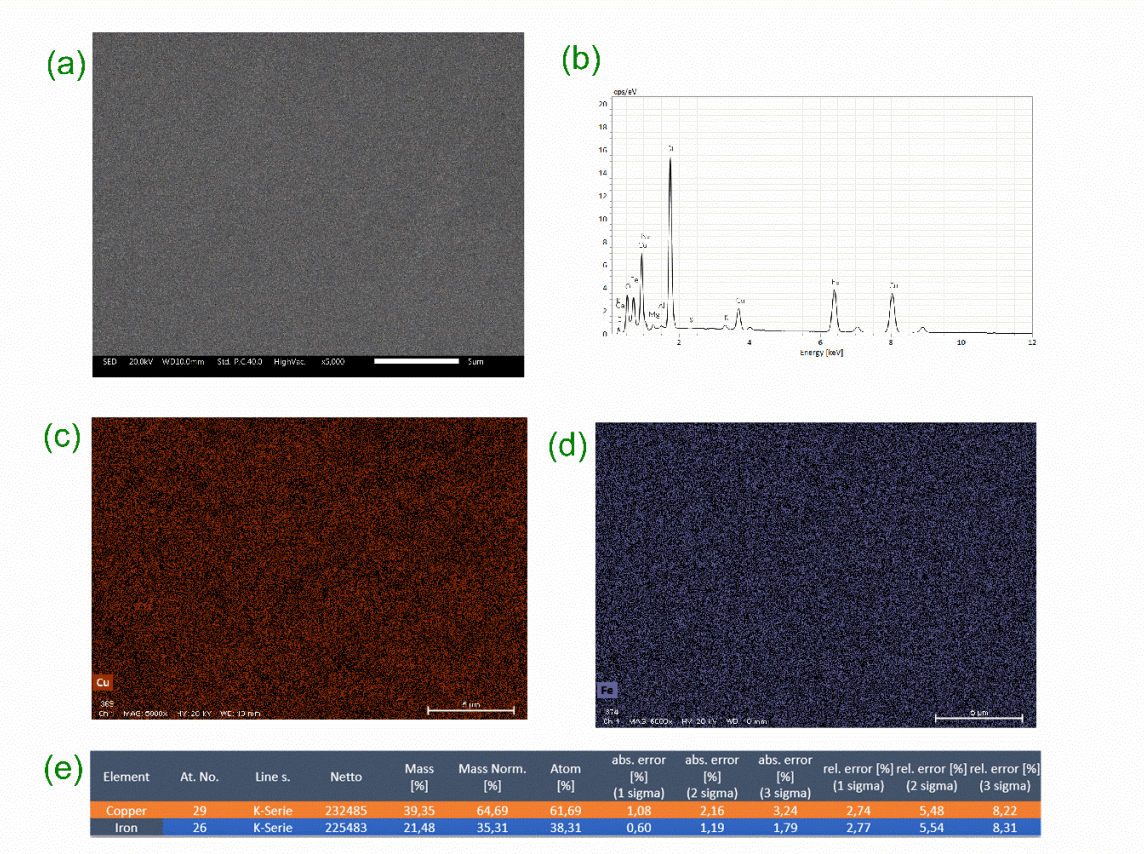

Element	At. No.	Line s.	Netto	Mass [%]	Mass Norm. [%]	Atom [%]	abs. error [%] (1 sigma)	abs. error [%] (2 sigma)	abs. error [%] (3 sigma)	rel. error [%] (1 sigma)	rel. error [%] (2 sigma)	rel. error [%] (3 sigma)
Copper	29	K-Serie	232485	39,35	64,69	61,69	1,08	2,16	3,24	2,74	5,48	8,22
Iron	26	K-Serie	225483	21,48	35,31	38,31	0,60	1,19	1,79	2,77	5,54	8,31

Figure S33. (a) SEM micrography with a magnification of 5000 times. (b) EDX performed in the same region of (a). (c) Chemical mapping of Cu and (d) chemical mapping of Fe using the same region of (a). (e) EDX element quantification analysis.

Supplementary Note S8: The morphological pattern of CFS

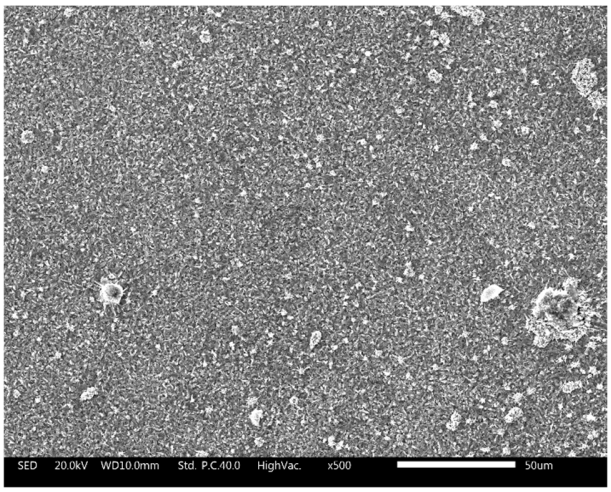

(a)

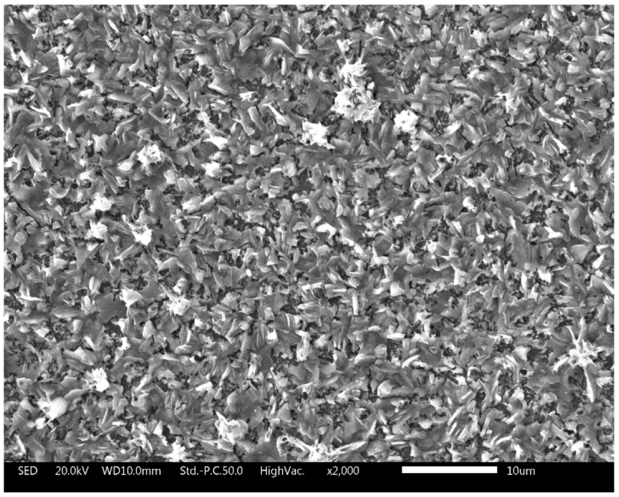

(b)

Figure S34. Micrographics of sample 18 obtained by SEM. (a) magnification of 500 times, (b) magnification of 2000 times.